


Peroxisome proliferator-activated receptor gamma coactivator 1-alpha protects a fibrotic liver from partial hepatectomy-induced advanced liver injury through regulating cell cycle arrest

Linzhong Zhang¹ | Wei Wang² | Lipeng Liu¹ | Yanghao Zhang¹ |
Xiuying Zhang¹ 

¹Department of Histology and Embryology, School of Basic Medical Sciences, Capital Medical University, Beijing, China

²Department of Urology, Beijing Chaoyang Hospital, Capital Medical University, Beijing, China

Correspondence

Dr Xiuying Zhang, Department of Histology and Embryology, School of Basic Medical Sciences, Capital Medical University, 10 Xi Tou Tiao, You An Men Wai, Beijing 100069, China.
Email: zhxy@ccmu.edu.cn; zhxy0515@hotmail.com

Funding information

National Natural Science Foundation of China, Grant/Award Number: 81470864

Abstract

Background: A fibrotic liver may have an impaired regenerative capacity. Because liver transplantation is donor limited, understanding the regenerative ability of a fibrotic liver is important.

Methods: A two-thirds partial hepatectomy (PH) was performed in C57Bl/6 mice with or without carbon tetrachloride (CCl₄) treatment. Liver regeneration in the fibrotic liver after PH was assessed by the intrahepatic expression of the cell cycle regulators p53, p21, cyclin D1, c-Fos and CDK2 using Western blot analysis. In addition, the expression of PGC-1 α and the cell proliferation-related proteins PCNA and phosphate histone H3 was determined by Western blot and immunohistochemical staining analyses. Histone epigenetic modification of the PGC-1 α promoter was investigated through chromatin immunoprecipitation (ChIP) and reverse transcription-quantitative polymerase chain reaction (RT-qPCR) assays. The impact of PGC-1 α on liver regeneration after PH was further evaluated in PGC-1 α -knockout mice.

Results: A decreased expression of PGC-1 α and liver regeneration-related genes in the fibrotic liver was detected after a PH. Histone acetylation at the PGC-1 α promoter led to increases in PGC-1 α expression and the survival rate in the fibrotic group after a PH. PGC-1 α -mediated liver regeneration was further demonstrated in PGC-1 α ^{f/f}albcre^{+/-0} mice.

Conclusion: Targeting PGC-1 α may represent a strategy to improve the treatment of PH in patients with liver fibrosis.

KEYWORDS

liver fibrosis, liver regeneration, oxidative stress, PGC-1 α

Linzhong Zhang, Wei Wang and Lipeng Liu contributed equally to this work.

This is an open access article under the terms of the Creative Commons Attribution-NonCommercial-NoDerivs License, which permits use and distribution in any medium, provided the original work is properly cited, the use is non-commercial and no modifications or adaptations are made.

© 2021 The Authors. *Basic & Clinical Pharmacology & Toxicology* published by John Wiley & Sons Ltd on behalf of Nordic Association for the Publication of BCPT (former Nordic Pharmacological Society).

1 | INTRODUCTION

Chronic liver injury, due to viral infection, ischaemia, alcohol or drug toxicity, often leads to fibrosis. This condition is characterized by excessive extracellular matrix (ECM) deposition in the periportal areas or the parenchyma and can advance to cirrhosis and hepatocellular carcinoma (HCC).¹ Cirrhosis precedes carcinoma in >75% of patients with primary HCC.² Hepatic resection is currently one of the curative treatments used to treat HCC. Nevertheless, patients with cirrhosis or HCC after resection tend to have a high risk of post-operative hepatic failure due to the insufficient regenerative ability of the remnant liver.

The liver is a unique organ with an enormous capacity for regeneration and restoration, both structurally and functionally, after extended resection or injury. However, it is clinically well known that the regeneration capacity of the liver is severely impaired in a fibrotic liver.³ Many published studies have focused on liver regeneration following a partial hepatectomy (PH) of a normal liver. Yet there have been few studies regarding fibrotic liver regeneration, and the mechanisms that are involved in the inefficient regeneration of a fibrotic liver remain unclear. Consequently, there are currently no treatment strategies or therapies that can improve the regeneration capacity of a fibrotic liver after resection.

Liver regeneration is a delicately orchestrated process that involves growth factors, inflammatory cytokines, cell cycle regulators and stem cells.^{4,5} The results of recent cell fate-tracing studies have suggested that mature hepatocytes can actively divide following a PH, whereas both intrahepatic and extrahepatic stem cells only contribute to liver regeneration when hepatocyte proliferation is impaired.⁶ A number of factors have been suggested to be associated with the impaired hepatocyte proliferation that is observed following a PH of a fibrotic or cirrhotic liver. Among them, p53, a known tumour-suppressor gene, has been shown to inhibit hepatocyte proliferation.⁷ However, p53-based regulation of the cell cycle during liver regeneration has not yet been investigated in a fibrotic liver after a PH. In addition, there are conflicting reports of hepatocyte proliferation following a PH in rodents with chronic hepatic injury. Several studies have suggested that there is a delayed peak in the cell cycle progression, whereas other studies have indicated immediate cell proliferation after a PH of cirrhotic rat livers.⁸⁻¹²

The peroxisome proliferator-activated receptor- γ coactivator-1 α (PPARGC1A or PGC-1 α) is a transcriptional coactivator that was initially identified as a peroxisome proliferator-activated receptor γ -interacting protein expressed in brown fat tissue.¹³ PGC-1 α also functions as

a strong transcriptional coactivator of p53 and facilitates the expression of many metabolic genes in response to nutritional and physiological stimuli as well as metabolic stress. Moreover, PGC1- α can bind to p53 and regulate its transactivation function, leading to the transactivation of proliferative and metabolic target genes.¹⁴ However, it is unknown whether the hepatic PGC1- α level is linked to impaired liver regeneration in a fibrotic liver.

Our previous studies, along with those of other researchers, have noted an increase in the level of reactive oxygen species (ROS) in the fibrotic liver. Therefore, we hypothesized that oxidant stress may lead to epigenetic inhibition of the PGC1- α expression in the fibrotic liver. A low level of PGC1- α induces a low level of p53, which inhibits cell cycle arrest and activates cell proliferation in the fibrotic liver at an early stage after PH. Cell cycle arrest is needed to create a checkpoint to allow for further accurate proliferation. Identification of the link between the PGC1- α and p53 levels and the regulation of cell proliferation may help develop effective strategies through which liver regeneration and clinical outcomes of patients with chronic liver disease can be improved following resection.

2 | MATERIALS AND METHODS

This study was conducted in accordance with the Basic & Clinical Pharmacology & Toxicology policy for experimental and clinical studies.¹⁵

2.1 | Cell culture and treatment

The human hepatic cell line L-02 (American Type Culture Collection, Manassas, VA, USA) was cultured in Dulbecco's modified Eagle's medium (DMEM; HyClone, Logan, UT, USA) supplemented with 10% (v/v) foetal bovine serum (Gibco, Carlsbad, CA, USA) and treated with 50-, 100-, 200-, 400- or 800- μ M H₂O₂ in a humidified environment (37°C with 5% CO₂). PGC-1 α expression was detected through reverse transcription-quantitative polymerase chain reaction (RT-qPCR) and Western blot assays. The primary hepatocytes were isolated from C57BL/6 mice according to our previously published protocol.¹⁶ Briefly, mice were anaesthetized with pentobarbital sodium (40 mg/kg) intraperitoneally. The liver was first perfused in situ through the portal vein with a calcium- and magnesium-free Hanks' balanced salt solution containing 0.5-mM EDTA and then digested with DMEM containing collagenase (Sigma-Aldrich, St. Louis, MO, USA) until the liver became soft

and loose. The digested liver was carefully dissected from the animal and placed in a dish where the collagenase digestion was continued at 37°C for an additional 10 min. The liver cell suspension was filtered and centrifuged at $50 \times g$ for 1 min, and the cell pellet was washed three times with DMEM in order to harvest the hepatocytes. L-02 cells and the primary hepatocytes were treated with 400- or 100- μM H_2O_2 , respectively, for 48 h. These cells were used for chromatin immunoprecipitation (ChIP) and quantitative RT-qPCR assays. The PGC-1 α CRISPR Activation Plasmid was purchased from Santa Cruz Biotechnology, and the PGC-1 α small interfering RNAs (siRNAs) and negative control siRNAs (Table S1) were purchased from Oligobio (Beijing, China). Cells were transfected with a PGC-1 α CRISPR activation plasmid or PGC-1 α siRNAs using Lipofectamine 2000 reagent (Invitrogen, USA), according to the manufacturer's instructions. After transfection for 24 h, the cells were cultured for 72 h and harvested for protein analysis of PGC-1 α , p53 and PCNA.

2.2 | Animal experiments

C57BL/6 mice (6-week-old males) were purchased from Beijing Vital River Laboratory Animal Technology Co., Ltd. (Beijing, China). The mice in the CCl_4 -treated groups were intraperitoneally injected with CCl_4 (1:9 in olive oil, Sigma) at a dose of 1-ml/kg body weight twice weekly for 6 or 8 weeks, whereas those in the control group were injected with the same volume of olive oil. Trichostatin A (TSA, Sigma, USA) at a dose of 0.6 mg/kg was intraperitoneally injected once a day for 1 week after the sixth or eighth week of CCl_4 administration, respectively. For the fibrosis + Mito-TEMPO group, the mice were treated with CCl_4 twice a week for 8 weeks, and 0.9% normal saline containing Mito-TEMPO (10 mg/kg) was injected intraperitoneally during the last 2 weeks every other day for 2 weeks. A two-thirds PH was performed 3 days after the final CCl_4 injection. This technique has been described previously in mice with pre-established liver fibrosis by CCl_4 .⁹ The mice were killed at 0 h, 6 h, 1 day, 2 days, 3 days, 5 days and 15 days after the PH, and the remnant hepatic tissues were harvested upon euthanization. Ppargc1 $\alpha^{f/f}$ (B6.Cg-Ppargc1 $\alpha^{\text{tm}2.1\text{Brsp}}/J$) and Tg (Alb-cre)^{21Mgn}/J (Alb-cre^{+/+}) mice were purchased from the Jackson Laboratory (Bar Harbor, ME, USA). The Alb-cre^{+/+} mice were crossed with C57BL/6 mice to generate Alb-cre^{+/-} mice. The Alb-cre^{+/-} mice were then crossed with Ppargc1 $\alpha^{f/f}$ mice to generate Ppargc1 $\alpha^{f/+}$ Alb-cre^{+/-} mice. Alb-cre^{0/0} mice (Ppargc1 $\alpha^{+/+}$) or hepatocyte-specific knockout mice (Ppargc1 $\alpha^{f/f}$ Alb-cre^{+/-}) were selected by crossing Ppargc1 $\alpha^{f/+}$ Alb-cre^{+/-}

and Ppargc1 $\alpha^{f/+}$ Alb-cre^{+/-} mice. AAV8-PGC-1 α (1.1×10^{12} transducing U/ml) and AAV8 (Hanbio, Shanghai, China) were intravenously delivered through the tail vein (100 μl per mouse) to Ppargc1 $\alpha^{f/f}$ Alb-cre^{+/-} mice. At 4 weeks after viral transduction, the liver tissues were collected for further experiments. Approximately 230 mice were used in the current study. All experimental procedures were conducted in accordance with the guidelines of Laboratory Animal Welfare Assurance issued by the US National Institutes of Health and were approved by the Animal Care and Use Committee of Capital Medical University.

2.3 | PH and evaluation of liver regeneration

Mice in both the CCl_4 -induced fibrotic and control groups were subjected to a two-thirds PH, as described previously.⁹ Briefly, mice were anaesthetized by an intraperitoneal injection of pentobarbital sodium (40 mg/kg). The median and left liver lobes were resected, respectively, distal to the 4-0 silk ties. The sham-operated animals did not undergo a PH. The body weight and survival of each mouse were recorded daily after surgery. The liver weight was determined upon sacrifice at 0 h, 6 h, 1 day, 2 days, 3 days, 5 days and 15 days after the PH to assess the liver regeneration parameters, as described previously.¹⁷ The levels of serum alanine aminotransferase (ALT) were measured to assess liver function using a metabolic kit (BioVision, Inc., Milpitas, CA, USA).

2.4 | Liver histopathology and immunohistochemistry

Haematoxylin and eosin (H&E) and Masson's staining were performed for histological evaluation. The PGC-1 α , p53, PCNA, 3'-nitrotyrosine and cleaved caspase-3 expression levels in liver tissues were estimated by immunohistochemistry using rabbit anti-PGC-1 α (1:1000; Abcam), mouse anti-p53 (1:200), mouse anti-PCNA (1:4000), mouse anti-3'-nitrotyrosine (1:1000; Life Technologies) or rabbit anti-cleaved caspase-3 (1:600; Cell Signaling Technology) antibodies. Commercially available human tissue arrays containing 10 normal liver tissues and 18 cirrhotic tissues (Cat No. LVD481 and LVC961) were purchased from the Shanghai Superbiotech Pharmaceutical Technology Co., Ltd. (Shanghai, China). The procedures followed were in accordance with the ethical standards of the responsible committee on human experimentation and with the 1975 Declaration of Helsinki, as

revised in 1983. The specimens were independently diagnosed by two pathologists.

2.5 | ChIP assay

A ChIP assay (ChIP assay kit, Thermo Fisher Scientific, Waltham, MA, USA) was performed on normal or fibrotic liver samples from the PH and sham groups as well as with H₂O₂-treated or untreated L-02 cells, as described previously with minor modifications.¹⁸ The protocol used was distinct from that used for the isolated cells. The tissue samples were homogenized after 37% formaldehyde cross-linking, according to the manufacturer's instructions. Anti-acetylated histone 3 polyclonal antibodies (Merck Millipore, Billerica, MA, USA) were added for immunoprecipitation. Finally, the purified DNA was used for qPCR detection with SYBR Green Master Mix (Applied Biosystems, CA, USA). The relative recruitment was calculated to be the amount of amplified DNA normalized to the input, relative to the values that were obtained from normal rabbit IgG immunoprecipitation, which were set as the background. An immunoprecipitated PGC1- α promoter sequence was quantified by qPCR with primers designed to amplify the region encompassing the 116 bp of the CRE site or an upstream region encompassing 160 bp outside the CREB response region (-430 bp).¹⁸ The primers for the PGC1- α CRE promoter region were as follows: forward, 5'-GGGC TGCCTTGAGTGACGTC-3' and reverse, 5'-AGTC CCCAGTCACATGACAAAG-3'; for the -430-bp promoter: forward, 5'-GCACACACATTTTAGGCAAGG-3' and reverse, 5'-TTTGAATGCCACCAACTCTAAACC-3'.

2.6 | Reverse transcription-quantitative polymerase chain reaction

Total RNA was extracted using TRIzol (Invitrogen Life Technologies, Carlsbad, CA, USA). cDNA was synthesized using total RNA templates by reverse transcription (PrimeScript 1st Strand cDNA Synthesis Kit, Takara Bio, Tokyo, Japan). qPCR was then performed using Power SYBR Green PCR Master Mix and the specific primers (listed in Table S1). The relative RNA level was determined using the comparative CT method ($2^{-\Delta\Delta CT}$).

2.7 | Western blot analysis

Liver tissue (40 mg) and L-02 cells were homogenized in lysis buffer (30-mM Tris, pH 7.5, 150-mM sodium

chloride, 1-mM phenylmethylsulfonyl fluoride, 1-mM sodium orthovanadate, 1% Nonidet P-40, 1% protease inhibitor cocktail [Sigma] and 10% glycerol) at 4°C. Approximately 40 μ g of protein extract from each sample was loaded onto a sodium dodecyl sulfate-polyacrylamide gel and separated by electrophoresis. The following primary antibodies were used: rabbit anti-PGC1- α antibody (1:2000; Invitrogen), mouse anti- α -smooth muscle actin (α -SMA) antibody (1:3000; Sigma), mouse anti-3'-nitrotyrosine antibody (1:2000; Life), mouse anti-p53 antibody (1:2000; Cell Signaling Technology), rabbit anti-p21 antibody (1:1000; Invitrogen), rabbit anti-cyclin D1 antibody (1:400; Invitrogen), mouse anti-PCNA antibody (1:2000; Cell Signaling Technology), rabbit anti-phospho-histone H3 antibody (1:2000; Cell Signaling Technology), rabbit anti-tumour necrosis factor- α (TNF- α) antibody (1:2000; Cell Signaling Technology), rabbit anti-interleukin-6 (IL-6) antibody (1:2000; Cell Signaling Technology), mouse anti-c-Fos antibody (1:3000; Abcam), rabbit anti-cyclin-dependent kinase (CDK) 1 antibody (1:2000; Abcam), rabbit anti-CDK2 antibody (1:2000; Abcam), rabbit anti-Flag antibody (1:1000; Invitrogen) and rabbit anti-cleaved caspase 3 antibody (1:2000; Cell Signaling Technology). The rabbit anti- β -actin antibody (1:4000; Cell Signaling Technology) and the rabbit anti-GAPDH antibody (1:4000, Cell Signaling Technology) were used as internal controls. Chemiluminescence (Bio-Rad, Hercules, CA, USA) was used to visualize protein bands, the density of which was quantified by densitometry.

2.8 | Terminal deoxynucleotidyl transferase dUTP nick end labelling method

Terminal deoxynucleotidyl transferase dUTP nick end labelling (TUNEL) staining was performed using an in situ Cell Death Detection Kit, POD (Roche Diagnostics, Mannheim, Germany), per the manufacturer's protocol. The average percentage of TUNEL-positive cells in five 400 \times fields served as an index of apoptosis.

2.9 | Statistical analyses

Statistical analyses were conducted with SPSS 12.0 software. GraphPad was used to export graphs. Variables are expressed as the mean \pm standard deviation. Comparisons were evaluated with the two-tailed Student's *t* test and analysis of variance (ANOVA). A *p* value <0.05 was considered statistically significant. Correlations between variables were evaluated using Pearson's *r*.

3 | RESULTS

3.1 | Cell proliferation occurs earlier in fibrotic livers after PH than in control livers

After CCl_4 treatment for 6 weeks, liver fibrosis was established (see Figure S1). The extent of liver regeneration in fibrotic and normal livers after a 70% PH was analysed, as shown in Figure 1. The survival rate of mice after a PH was significantly lower in the fibrotic group than that observed in the control group (Figure 1A). The body weight of mice was reduced following a PH compared with the weight before a PH in both the fibrotic and control groups. However, the weight loss that was noted in the fibrotic mice was greater than that observed in the control mice (Figure 1B). In addition, the serum ALT levels in the fibrotic group after a PH were greater than those of the control group (Figure 1C). This difference might be caused by a higher level of severity of liver injury that further aggravated the existing injury, as characterized by the higher levels of hepatocyte necrosis and apoptosis observed in the fibrotic livers at Day 1, Day 3 and reaching the second peak at Day 5 after PH (Figure 1D,E). However, compared with the results observed in the control group, the hepatic PCNA and phospho-histone H3 expression levels were higher in the fibrotic group at 1 day after PH, but lower at Days 2 and 3, which were associated with a lower liver weight (Figure 1F,G). Additionally, the baseline PCNA and phospho-histone H3 levels were high in the fibrotic mice. These results were associated with the pathological features of fibrotic livers, that is, the coexistence of degenerative and necrotic hepatocytes and the proliferation of hepatocytes and nonparenchymal cells (Figure S1), suggesting an ongoing pathological process in fibrotic livers. Moreover, the cleaved caspase-3 expression was higher in the fibrotic group than in the control group (Figures S2 and S3). These results suggest that hepatocyte proliferation occurred earlier in the fibrotic livers than in the control livers after a PH. However, this proliferation was quickly followed by a higher level of apoptosis and necrosis as well as a reduced level of regeneration than the levels observed in the control group.

3.2 | Oxidative stress decreases PGC-1 α expression, moderates the p53 level and disturbs the cell cycle arrest in fibrotic livers after a PH

To characterize the possible mechanisms involved in the inefficient liver regeneration that is observed in fibrotic

livers, we evaluated the function of p53, a well-known tumour-suppressor gene, in the regulation of hepatocyte proliferation during liver regeneration. Although the level of p53 was higher in the fibrotic group than in the control group at an earlier time after PH, which could be carryover from a higher baseline level in fibrotic livers, the p53 level was significantly lower in the fibrotic group than in the control group at 24 h after PH (Figure 2A). Next, we measured the level of p21, a downstream mediator of p53 that is related to the regulation of cell cycle arrest, as shown in Figure 2A. The level of p21 was lower in the fibrotic group than in the control group at 24 h after PH. However, the expression levels of cyclin D1, CDK2, c-Fos, phospho-histone H3 and PCNA (Figures 1F and 2A), which reflect activation or progression of the cell cycle and cell proliferation, were higher in the fibrotic group than in the control group at 24 h after PH. This result confirmed the inhibition of cell cycle arrest in the fibrotic liver. Next, we hypothesized that the observed decreased p53 expression in the fibrotic livers at 24 h after PH might be caused by the lower level of PGC-1 α , because the baseline level of p53 was higher in the fibrotic liver before the PH than the level observed in the control group (Figure 2A). It is known that PGC-1 α functions as a p53 coactivator,¹⁹ as evidenced by the results from the *in vitro* transfection with the PGC-1 α activation plasmid in Figures 2B and S4. Enhanced PGC-1 α expression led to increased p53 expression and decreased PCNA expression. In this study, the expression of PGC-1 α was lower in the fibrotic liver before the PH and at 24 h after PH than in the control group (Figure 2A). We then investigated whether the lower expression of PGC-1 α was induced by an increased level of oxidative stress. This hypothesis was tested using 3'-nitrotyrosine. ROS react with nitric oxide, generating peroxynitrite (which binds to protein residues such as tyrosine to yield nitrotyrosine), and nitrotyrosine is considered to be a biological marker of oxidative stress.²⁰ Higher 3'-nitrotyrosine and lower PGC-1 α expression levels were detected in human cirrhotic livers compared with the levels observed in normal livers. This result indicates an association between oxidative stress and PGC-1 α inhibition (Figure 2C). The level of 3'-nitrotyrosine was higher in the fibrotic group, before and after the PH, than in the control group (Figure 2D). To further test this hypothesis, Mito-TEMPO, an inhibitor of oxidative stress, was used to evaluate the role of oxidative stress on PGC-1 α expression by Western blot. Mito-TEMPO significantly reduced the levels of 3'-nitrotyrosine and α -SMA in the livers of mice that were treated with CCl_4 for 6 weeks. Simultaneously, the reduction in PGC-1 α and p53 expression was reversed under Mito-TEMPO conditions (Figure 2E). *In vitro* studies further confirmed that PGC-1 α expression

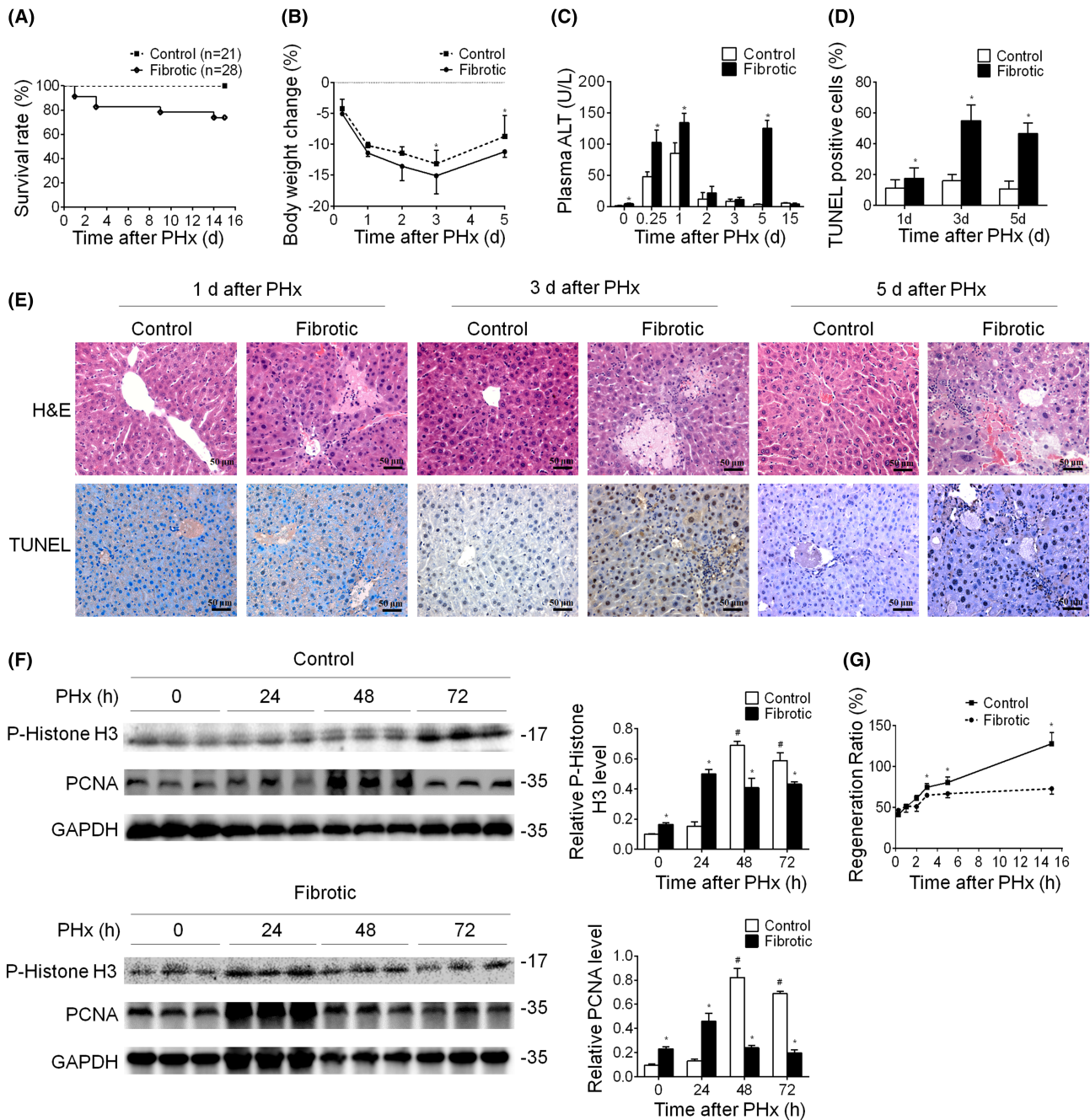


FIGURE 1 Tissue injury and cell proliferation are promoted early after PH in fibrotic livers. (A) The mouse survival rates over time. The survival rate was calculated using the Kaplan–Meier method, $n = 21$ for the control group and $n = 28$ for the fibrotic group, $p < 0.05$ versus the control mice. (B) Body weight loss curves at Days 1, 2, 3 and 5 after PH, expressed as a per cent change in individual mouse body weight using the pre-PH body weight as a reference (means \pm SEM), $p < 0.05$ versus the control mice. (C) Plasma levels of ALT. Means \pm SEM, $p < 0.05$ versus the control mice. (D, E) H&E and TUNEL assays in liver sections harvested at Days 1, 3 and 5 after PH in both groups (magnification, 20 \times). (D) TUNEL-positive nuclei were counted in 10 high-power fields of each section for ≥ 5 mice per time point. Each bar represents means \pm SEM of the number of positive nuclei in a high-power field. $*p < 0.05$ versus the control mice. (F) The protein levels of PCNA and phospho-histone H3 were detected at 0, 24, 48 and 72 h after PH by Western blot. GAPDH was used as an internal control. $*p < 0.05$ versus the control group ($\#p < 0.05$). (G) The regeneration ratio is expressed by dividing the final liver weight at sacrifice by the estimated remnant liver weight. Data are expressed as means \pm SEM, as described in Section 2. $*p < 0.01$ compared with the control mice at each time point. For (B)–(G), $n = 4$ mice in each group; experiments were repeated at least three times. The total number of animals in each group was approximately 12. Analyses were performed using the unpaired t test (B, C, D, G) and two-way ANOVA (F)

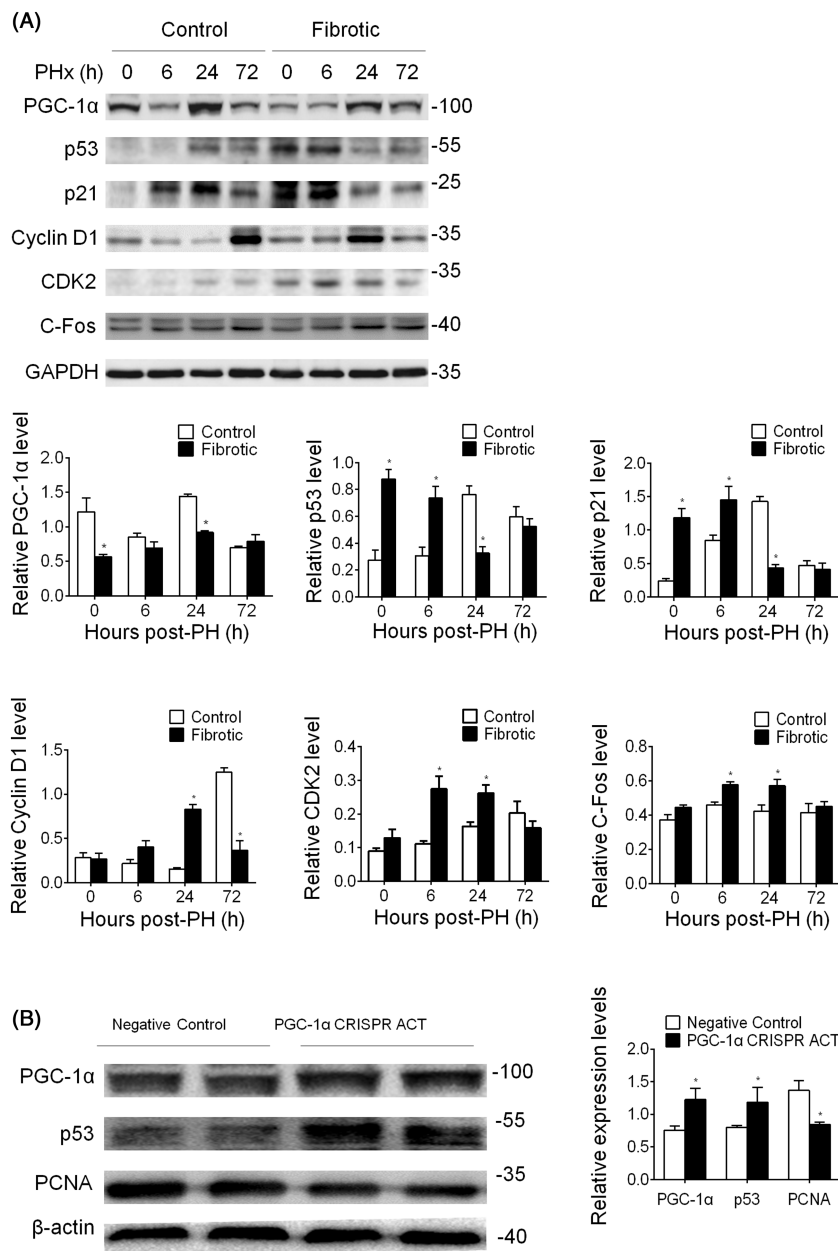


FIGURE 2 Enhanced oxidative stress inhibited the expression of PGC-1 α and p53 and promoted the cell proliferation in fibrotic livers after a PH. (A) Comparison of the cell cycle-related protein expression levels in fibrotic livers after a PH. The PGC-1 α , p53, p21, cyclin D1, CDK2 and c-Fos protein levels were detected by Western blot in CCl₄-treated and control groups at 6, 24 and 72 h after PH, respectively. GAPDH was used as an internal control. A representative blot is shown, * $p < 0.05$, unpaired t test. (B) Western blot analysis of PGC-1 α , p53 and PCNA in L-02 cells after transfection with the PGC-1 α CRISPR activation plasmid or negative control plasmid. A representative blot from three independent transfections is shown, * $p < 0.05$, unpaired t test (PGC-1 α CRISPR ACT: PGC-1 α CRISPR activation plasmid). (C) H&E and immunohistochemical staining of 3'-nitrotyrosine and PGC-1 α in normal human liver ($n = 10$) and cirrhotic ($n = 18$) tissues (magnification, 20 \times). Correlation of PGC-1 α expression with the 3'-nitrotyrosine level. (D) The enhancement of oxidative stress in fibrotic livers after a PH. The protein level of 3'-nitrotyrosine was determined by Western blot at 24 h after PH; GAPDH was used as an internal control. * $p < 0.05$, unpaired t test. (E) Mito-TEMPO was employed to reverse the effect of oxidative stress on the levels of 3'-nitrotyrosine, PGC-1 α , p53 and α -SMA, as detected by Western blot analysis. GAPDH was used as a loading control. * $p < 0.05$, unpaired t test. For (A), (D) and (E), $n = 4$ mice in each group; experiments were repeated at least three times. The total number of animals in each group was approximately 12. (F) H₂O₂ administration inhibited the expression of PGC-1 α in vitro. PGC-1 α expression was detected by Western blot after L-02 cells were treated with 0-, 50-, 100-, 200-, 400- or 800- μ M H₂O₂, respectively. β -Actin was used as an internal control. * $p < 0.05$, unpaired t test; data represent at least four independent treatments

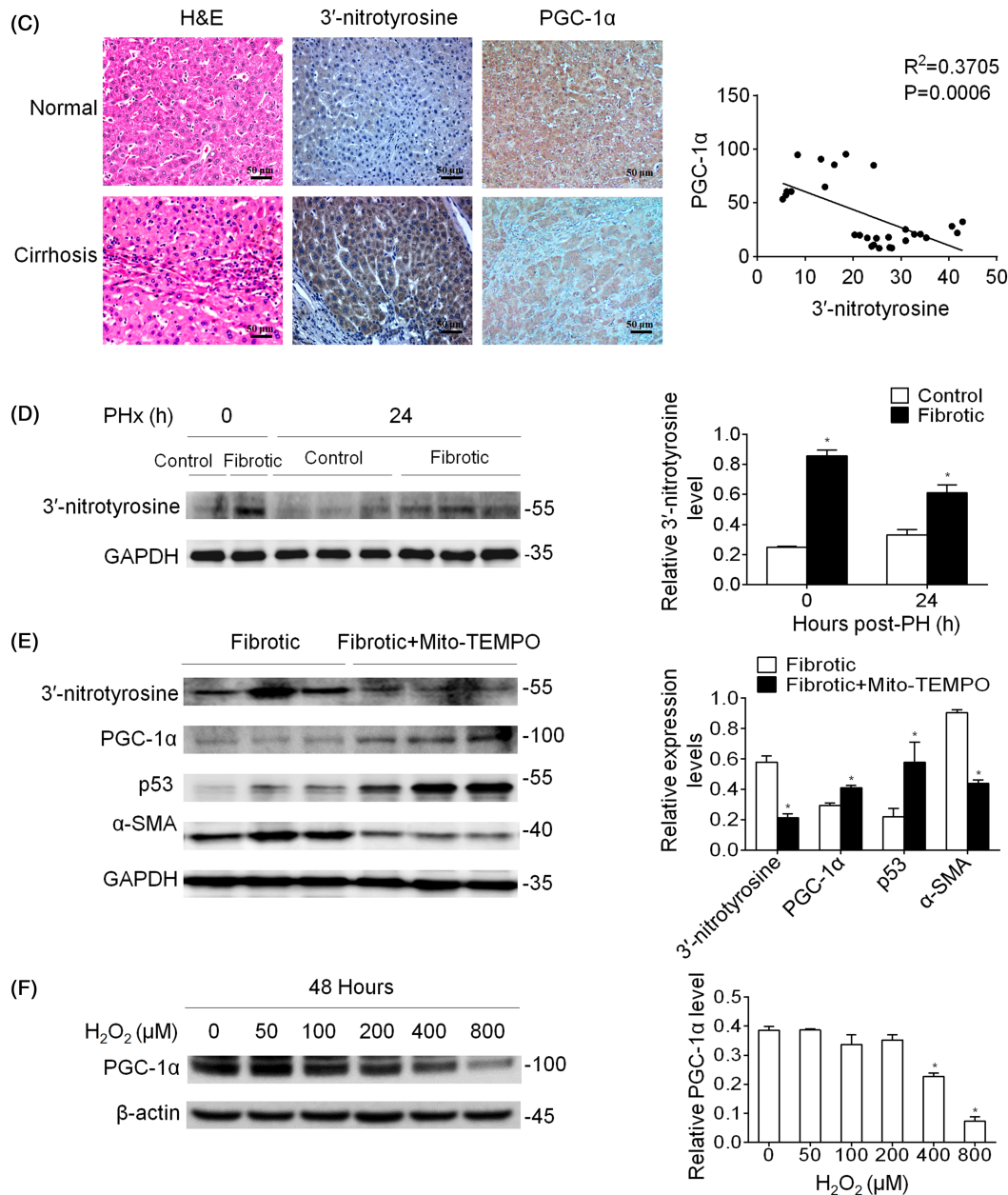


FIGURE 2 (Continued)

was also decreased after H₂O₂ treatment in L-02 cells (Figure 2F). These results indicate that oxidative stress can repress p53 expression through inhibition of the expression of its coactivator, PGC-1α, and attenuate cell cycle arrest. As indicated by our previous study,²¹ cell cycle arrest permits time for subsequent accurate cellular replication. However, impaired cell cycle arrest led to a higher level of cell injury in fibrotic livers than in control livers following a PH. In addition, the levels of the pro-inflammatory cytokines TNF-α and IL-6, which have been suggested to be involved in hepatocyte priming after PH,²² were increased in both the fibrotic livers and the control group after a PH. These levels were higher in the

fibrotic livers than in the control group (Figure S2). This may further promote hepatocyte priming earlier after PH in the fibrotic liver.

3.3 | Oxidative stress decreases PGC-1α expression through epigenetic modification of the PGC-1α promoter

Subsequently, we investigated whether oxidative stress induced the inhibition of histone acetylation at the starting site of the PGC-1α gene.¹⁸ In vitro studies showed that the level of PGC-1α histone H3 acetylation

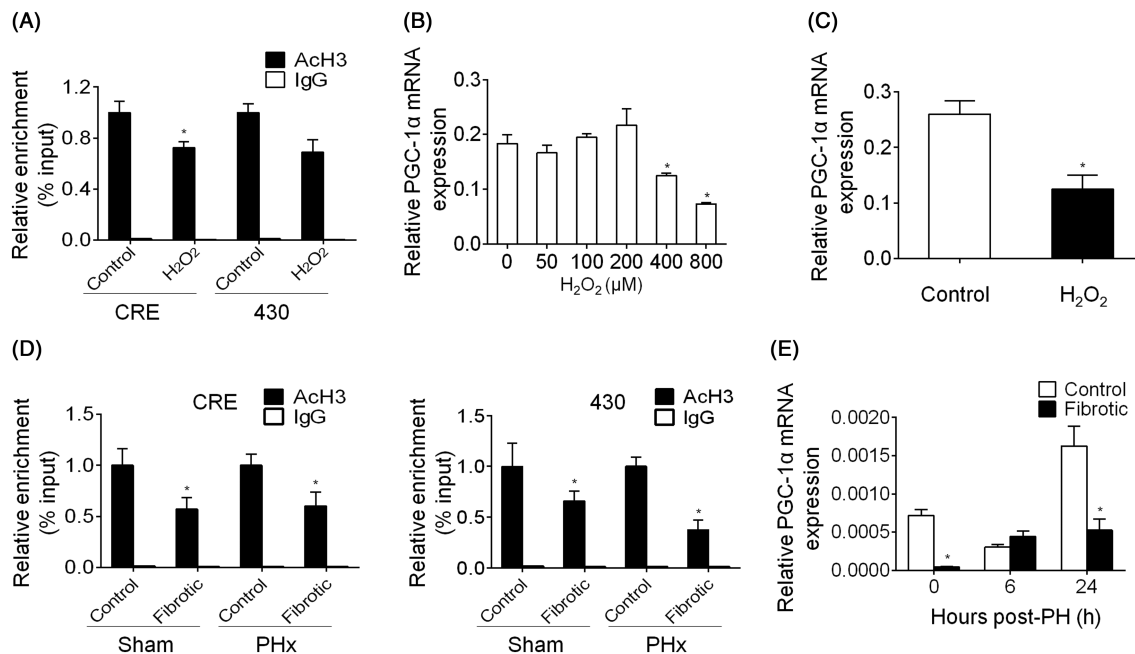


FIGURE 3 Oxidative stress inhibited PGC-1 α expression by deacetylation of histone in the PGC-1 α promoter region. (A) ChIP analysis of the CRE and -430-bp sites in the PGC-1 α proximal promoter in L-02 cells after H₂O₂ treatment. Graphs show qPCR values normalized to the input DNA ($p < 0.05$). AcH3, H3 acetylation; IgG, immunoglobulin. (B) PGC-1 α expression was detected by RT-qPCR after L-02 cells were treated with 0-, 50-, 100-, 200-, 400- or 800- μ M H₂O₂, respectively. $p < 0.05$. (C) RT-qPCR analysis of PGC-1 α transcription in primary hepatocytes after 100- μ M H₂O₂ treatment for 48 h ($p < 0.05$). For (A)–(C), data represent at least four independent treatments. (D) A decline in the histone H3 acetylation in fibrotic livers at 24 h after PH was detected at both the CRE and -430-bp sites compared with the results of the control livers. The RT-qPCR values after normalization to the input DNA are shown ($p < 0.05$). (E) A significant decrease in the expression of PGC-1 α mRNA was determined in fibrotic livers after PH by RT-qPCR. $p < 0.05$ versus the control group ($p < 0.05$). For (A), (D) and (E), $n = 4$ mice in each group; experiments were repeated at least three times. The total number of animals in each group was approximately 12. For (A)–(E), comparisons were evaluated with unpaired t test

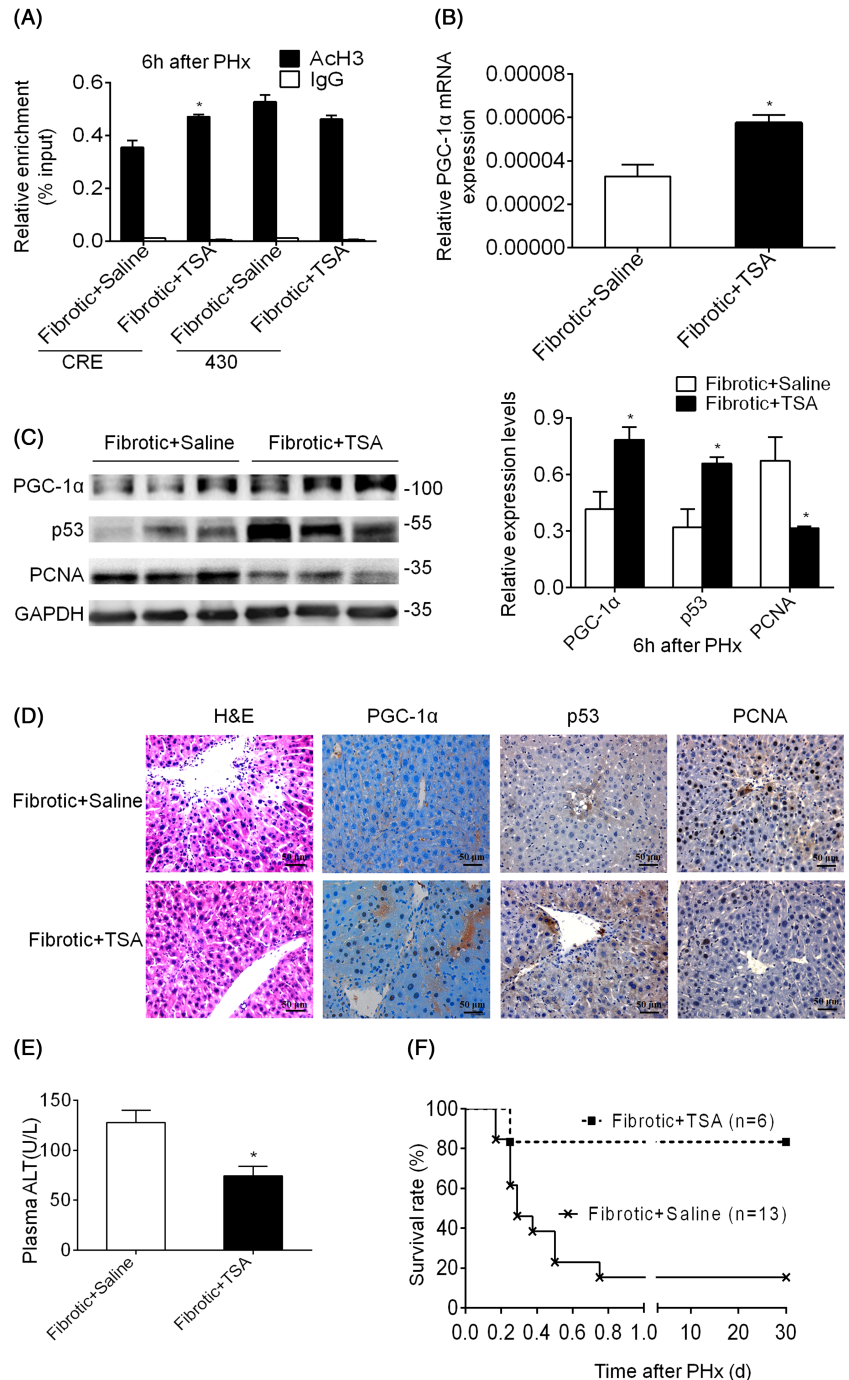
at the CRE site in L-02 cells was decreased following H₂O₂ treatment (Figure 3A). Consequently, the mRNA level of PGC-1 α was markedly reduced in L-02 cells and primary hepatocytes that were treated with H₂O₂ (Figure 3B,C). In addition, the results from the in vivo studies showed that level of H3 acetylation was lower in the fibrotic livers of both the sham and PH groups in the region that is located 430-bp upstream of the transcription start site and the CRE region compared with the results observed in the control livers (Figure 3D). As a result, the PGC-1 α mRNA level was lower in the fibrotic livers than in the control livers (Figure 3E).

3.4 | Histone acetylation of the PGC-1 α promoter reverses p53-induced cell cycle arrest in the fibrotic liver

TSA, a histone deacetylase inhibitor (HDACi),^{23,24} was used to investigate the role of PGC-1 α in cell cycle arrest in the fibrotic liver after PH. The ChIP assay results showed that the histone H3 acetylation levels at the CRE

site of the PGC-1 α promoter were higher in the fibrotic + TSA group than in the fibrotic group after PH (Figure 4A). This was also confirmed by the results of the RT-qPCR analysis (Figure 4B). Subsequently, there was a marked increase in the protein level of PGC-1 α , followed by an increase in the p53 expression and a sharp decrease in the PCNA expression (Figure 4C). This finding indicates that histone H3 acetylation at the PGC-1 α promoter led to the increase in PGC-1 α expression as well as cell cycle arrest. To investigate the protective function of PGC-1 α in severe liver injury, mice were treated with CCl₄ for 8 weeks, followed by TSA treatment for 1 week. At post-operative Day 1, the H&E and immunohistochemical staining results showed a significant improvement in the liver morphology, accompanied by PGC-1 α nuclear translocation and cell cycle arrest (Figure 4D). Furthermore, the serum ALT level and survival rate in the fibrotic group after a PH were significantly improved in the animals that underwent this treatment protocol than in those that did not (Figure 4E, F). These results indicate that epigenetic inhibition of PGC-1 α expression in fibrotic livers leads to a decreased

FIGURE 4 Histone acetylation of the PGC-1 α promoter reversed p53-induced cell cycle arrest in fibrotic livers. (A) ChIP analysis of the CRE and -430-bp sites in the PGC-1 α proximal promoter was performed at 6 h after PH in fibrotic livers with or without TSA treatment. The qPCR values after normalization to the input DNA and relative to the NaCl-treated mice are shown ($*p < 0.05$). AcH3, H3 acetylation; IgG, immunoglobulin. (B) PGC-1 α mRNA was determined by RT-qPCR in fibrotic livers at 6 h after PH, which were pretreated with TSA or saline for 1 week. *Versus the control group ($*p < 0.05$). (C) Representative Western blotting analysis of PGC-1 α , p53 and PCNA protein expression in fibrotic livers at 6 h after PH, which were pretreated with TSA or saline for 1 week. Quantifications were normalized to GAPDH ($*p < 0.05$). H&E staining and immunohistochemical staining of PGC-1 α , p53 and PCNA (magnification, 20 \times) (D), plasma levels of ALT (E) at Day 1 after PH and survival rates (F) of mice following 8 weeks of CCl $_4$ treatment in fibrotic livers, which were pretreated with TSA or saline for 1 week. $P < 0.05$ versus the control mice. For (A)–(E), $n = 4$ mice in each group; experiments were repeated at least three times. The total number of animals in each group was approximately 12. For (A), (B), (C) and (E), comparisons were evaluated with unpaired t test



p53 level, which inhibits cell cycle arrest and leads to more injury after PH.

3.5 | Impaired liver regeneration in PGC-1 α ^{f/f}albcre^{+/-0} (LKO) mice

To investigate the regulatory function of PGC-1 α in liver regeneration, LKO mice were used. In these mice, the PGC-1 α gene was selectively knocked out in hepatocytes. The survival rate of the LKO mice was significantly lower

than that of wild-type mice following a PH (Figure 5A). The serum ALT levels and TUNEL-positive cells in the LKO mice after a PH were higher than those of the wild-type mice (Figure 5B,C). H&E staining revealed many small areas of necrosis in the LKO mice (Figure 5C). The impact of PGC-1 α was further confirmed by a decrease of p53 expression and an increase of PCNA expression, accompanied by higher cleaved caspase-3 expression levels at 6 h after PH in the LKO mice compared with the results observed in the wild-type group, as demonstrated by the immunohistochemical staining and Western blot

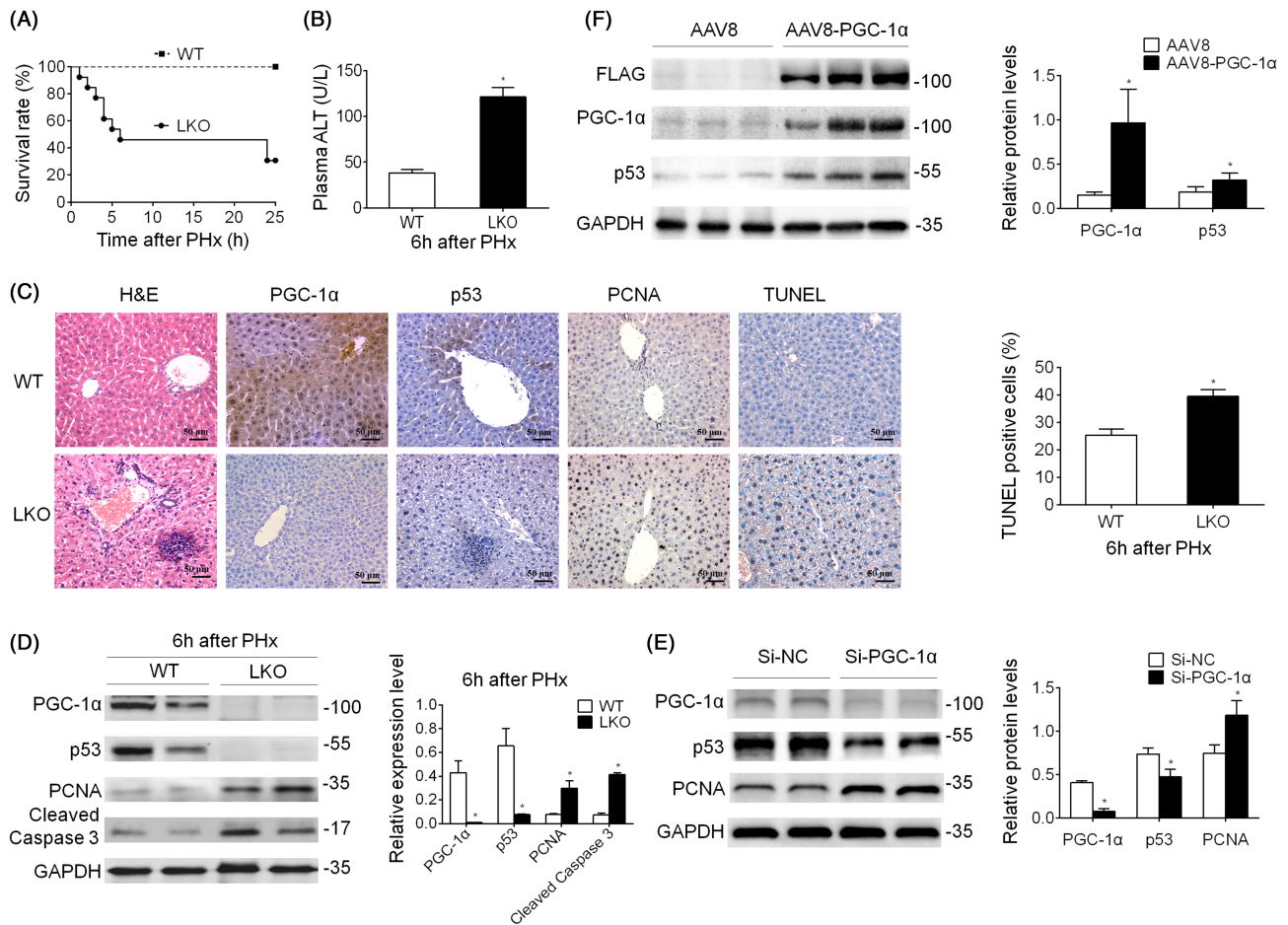


FIGURE 5 PGC-1 α affected cell proliferation. (A) Survival rates of PGC-1 $\alpha^{f/f}$ albcre $^{+/0}$ and wild-type mice after PH. ($p < 0.01$, $n = 12$ in each group). (B) Plasma levels of ALT. $^*p < 0.05$. (C) H&E staining, TUNEL staining and immunohistochemical staining of PGC-1 α , p53 and PCNA in PGC-1 $\alpha^{f/f}$ albcre $^{+/0}$ mice and wild-type mice after a PH (magnification, 20 \times). $^*p < 0.05$. (D) Protein levels of PGC-1 α , p53, PCNA and cleaved caspase 3 in PGC-1 $\alpha^{f/f}$ albcre $^{+/0}$ mice and wild-type mice after a PH as detected by Western blot analysis, $^*p < 0.05$. LKO, hepatocyte-specific PGC-1 $\alpha^{f/f}$ albcre $^{+/0}$ mice; WT, wild-type mice. For (B)–(D), $n = 4$ mice in each group; experiments were repeated at least three times. The total number of animals in each group was approximately 12. (E) Western blot analysis of PGC-1 α , p53 and PCNA in mouse primary hepatocytes after transfection with si-PGC-1 α or si-NC; a representative blot from three independent transfections is shown, $^*p < 0.05$. (F) The protein levels of Flag, PGC-1 α and p53 in liver tissues from the AAV8 empty vector group and AAV8-PGC-1 α administration group were determined by Western blot analysis. $^*p < 0.05$ versus the AAV8 empty vector group. Data represent the mean \pm SEM, $n = 8$. AAV8 represents the AAV8 empty vector administration group, and AAV8-PGC-1 α represents the AAV8-PGC-1 α administration group. For (B)–(F), comparisons were evaluated with unpaired t test

analyses (Figure 5C,D). To further confirm that PGC-1 α is necessary for p53 protein expression, PGC-1 α siRNA was transfected into mouse primary hepatocytes. A lower PGC-1 α expression led to decreased p53 expression and increased PCNA expression (Figure 5E). Moreover, the adeno-associated virus serotype 8 (AAV8) vector carrying PGC-1 α was utilized. The infection efficiency of AAV8-PGC-1 α was observed by Western blot with the Flag protein in order to confirm the successful delivery of PGC-1 α , and PGC-1 α was found to be overexpressed in the mouse liver. Compared with the AAV8 empty vector-transfected LKO mice, the AAV8-PGC-1 α -administered mice exhibited increased p53 expression as confirmed by

Western blot (Figure 5F), indicating that PGC-1 α is necessary for p53 expression. These results further illustrate that the reduced PGC-1 α expression is linked to impaired liver regeneration, possibly through the disturbed cell cycle arrest after PH.

4 | DISCUSSION

In this study, we employed both in vivo and in vitro systems to investigate why liver regeneration is less efficient in fibrotic livers than in healthy livers following a two-thirds PH. We investigated the PGC-1 α -regulated p53

pathways in liver regeneration and found that oxidative stress downregulated the expression of PGC-1 α , moderated the p53 level and inhibited the cell cycle arrest in fibrotic livers. These factors appear to be responsible for the reduced liver regeneration that is observed in fibrotic livers after a PH.

Liver regeneration is a delicately orchestrated yet complex process that can fully restore the lost tissue mass after a normal liver is resected by a volume of two thirds. Liver regeneration after injury or resection mainly depends on the proliferation of hepatocytes. In this study, we first investigated liver injury and hepatocyte proliferation in fibrotic livers after a PH. The histological results revealed that a PH aggravated the liver injury in fibrotic livers and led to a reduction in body weight, both of which led to a higher rate of mortality in this group than in the control group (Figure 1). At post-operative Day 1, cell proliferation appeared to be increased in the fibrotic group compared with that of the control group. However, by post-operative Day 3, the level of proliferation in the fibrotic group was lower and the level of apoptosis was higher compared with the results of the control group. A second peak in hepatic injury was observed at Day 5 after PH, as evidenced by higher serum ALT, hepatic necrosis and apoptosis levels than observed in the control group (Figures 1 and S3). These findings were consistent with those of a previous study.⁹ Cell proliferation is regulated by many cellular proteins and cell signalling transduction pathways, including the p53–p21 pathway. It appears that inhibition of the p53–p21 pathway promotes cell proliferation and that activation of the same pathway suppresses proliferation in liver regeneration.²⁵ The impaired liver regeneration observed in cirrhotic livers was accompanied by a reduction in the cyclin D1 expression and Akt phosphorylation as well as the upregulation of p53 and p21Cip1 expression.²⁶ However, our results suggest that no significant cell cycle arrest was detected and that proliferation in the fibrotic liver was immediately initiated after the PH. As for the cause of the changes in cell proliferation in the fibrotic liver after a PH, we speculate that it could be related to the expression of p53. In our study, p53 expression was lower in the fibrotic livers than in the control livers at 24 h after the PH. This may inhibit cell cycle arrest, leading to the activation of cell proliferation (Figures 1F and 2A). p53 downregulated the expression of cell cycle proteins, including various cyclins and CDKs. As a CDK inhibitor, the p53–p21 pathway can induce cell cycle arrest at several stages, including the G₁/S and G₂/M checkpoints, by inhibiting CDK complexes.^{27–30} p53 can induce G₁/S arrest via p53–p21-dependent inhibition of cyclin E–CDK2.³¹ The current study demonstrated that cyclin D1 and CDK2 expression was higher at an earlier

time point in fibrotic livers compared with the results of the parallel control livers after PH, due to inhibition of the p53–p21 pathway (Figure 2A). This finding suggests that there was inhibition of cell cycle arrest at the G₁/S checkpoint. Induction of cyclin D1 is considered to be the best marker for the G₁-to-S transition in the regenerating liver.³² However, in this study, there were no significant differences in the CDK1 expression levels between the two groups, suggesting that inhibition of cell cycle arrest was not at the G₂/M checkpoint (Figure S2). Cell cycle arrest is required for base excision and the repair of oxidized and injured DNA after a PH. Inhibition of cell cycle arrest leads to earlier but faulty cell proliferation, finally resulting in necroptosis and ineffective regeneration of the fibrotic liver. Additionally, the G₀-to-G₁ transition in hepatocytes after a PH is induced by TNF- α and IL-6.^{22,33,34} Our results show that the expression of these cytokines was significantly increased in both the fibrotic and control livers after PH. However, this increase was significantly greater in the fibrotic livers than in the controls (Figure S2). Overstimulation of TNF- α can lead to the intracellular production of ROS and lipid peroxidation, which are known to follow a PH.³⁵ This would further aggravate hepatocyte impairment and result in the ineffective regeneration capacity of the fibrotic liver.

In addition, the immediate-early gene c-Fos plays a pivotal role in the priming phase of liver regeneration. c-Fos may be induced by the IL-6/Stat3 pathway during liver regeneration.³⁶ In the current study, the expression of c-Fos was elevated in fibrotic livers at 24 h after PH. Thus, we speculate that this elevated c-Fos expression might be caused by the higher level of IL-6 (Figure S2). However, other studies have shown that the level of c-Fos increases at a much earlier time point, with reports of an elevation in the level of c-Fos at 1 h after PH³⁷ because it is an immediate-early gene.

Hepatic oxidative stress is expected to be exacerbated by a PH of fibrotic livers. PGC-1 α , which functions as the coactivator of p53, is a member of a small family of transcriptional factors that regulate the expression of genes involved in oxidative stress, mitochondrial metabolism and biogenesis.³⁸ In this study, the expression of PGC-1 α was suppressed by oxidative stress, as shown by the analysis of human liver samples both in vivo and in vitro. The finding that PGC-1 α regulates cell proliferation was further supported by the use of PGC-1 α LKO mice (Figure 5). Our results represent the first study to demonstrate that increased oxidative stress in fibrotic livers alters the expression of PGC-1 α through epigenetic modification, leading to a decrease in the p53 level and activation of cell proliferation at an early stage after PH.

The conformation of chromatin is subject to regulation through histones and their covalent modifications to

respond to the transcription status.^{39–41} Post-translational covalent modifications (acetylation, phosphorylation and methylation) of histones at the NH₂-terminal tail create regulatable contacts with the underlying DNA. Thus, histone modifications regulate gene expression.⁴² Acetylation of H3 is generally considered a key step towards the activation of transcribed genes.^{43,44} PGC-1 α acetylation and function also appear to rely on a delicate balance between the histone acetyltransferase HAT and histone deacetylases. This study shows that the H3 acetylation at the PGC-1 α promoter region in fibrotic livers was low both before and after a PH. The restriction of H3 acetylation was relieved using the HDACi TSA, which altered the epigenetic conformation at the PGC-1 α region, thus activating PGC-1 α transcription in this study. Our findings indicate that the H3 deacetylation status at the PGC-1 α promoter region caused by oxidative stress in fibrotic livers results in the downregulation of PGC-1 α expression before and after a PH.

In conclusion, the inefficient regeneration observed in fibrotic livers after PH was associated with an altered PGC-1 α level. Furthermore, the expression of PGC-1 α can be epigenetically regulated, which suggests that this is a possible pathway through which to develop new therapies for the improvement of liver regeneration in fibrotic livers.

ACKNOWLEDGEMENT

This work was supported by the National Natural Science Foundation of China, Award Number 81470864.

CONFLICT OF INTERESTS

All the authors declare no competing interests.

ORCID

Xiuying Zhang  <https://orcid.org/0000-0002-2120-0832>

REFERENCES

- Massarweh NN, El-Serag HB. Epidemiology of hepatocellular carcinoma and intrahepatic cholangiocarcinoma. *Cancer Control*. 2017;24(3):1073274817729245.
- Nagasue N, Kohno H, Chang YC, et al. Liver resection for hepatocellular carcinoma. Results of 229 consecutive patients during 11 years. *Ann Surg*. 1993;217(4):375-384.
- Llovet JM, Burroughs A, Bruix J. Hepatocellular carcinoma. *Lancet*. 2003;362(9399):1907-1917.
- Fausto N, Campbell JS, Riehle KJ. Liver regeneration. *Hepatology*. 2006;43(2 Suppl 1):S45-S53.
- Gilgenkrantz H, Collin de l'Hortet A. Understanding liver regeneration: from mechanisms to regenerative medicine. *Am J Pathol*. 2018;188(6):1316-1327.
- Malato Y, Naqvi S, Schurmann N, et al. Fate tracing of mature hepatocytes in mouse liver homeostasis and regeneration. *J Clin Invest*. 2011;121(12):4850-4860.
- Stepniak E, Ricci R, Eferl R, et al. c-Jun/AP-1 controls liver regeneration by repressing p53/p21 and p38 MAPK activity. *Genes Dev*. 2006;20(16):2306-2314.
- Kato A, Bamba H, Shinohara M, et al. Relationship between expression of cyclin D1 and impaired liver regeneration observed in fibrotic or cirrhotic rats. *J Gastroenterol Hepatol*. 2005;20(8):1198-1205.
- Kuramitsu K, Sverdlov DY, Liu SB, et al. Failure of fibrotic liver regeneration in mice is linked to a severe fibrogenic response driven by hepatic progenitor cell activation. *Am J Pathol*. 2013;183(1):182-194.
- Revuelta-Cervantes J, Mayoral R, Miranda S, et al. Protein tyrosine phosphatase 1B (PTP1B) deficiency accelerates hepatic regeneration in mice. *Am J Pathol*. 2011;178(4):1591-1604.
- Xiong Y, Torsoni AS, Wu F, et al. Hepatic NF-kB-inducing kinase (NIK) suppresses mouse liver regeneration in acute and chronic liver diseases. *Elife*. 2018;7.
- Makino H, Shimizu H, Ito H, et al. Changes in growth factor and cytokine expression in biliary obstructed rat liver and their relationship with delayed liver regeneration after partial hepatectomy. *World J Gastroenterol*. 2006;12(13):2053-2059.
- Puigserver P, Wu Z, Park CW, Graves R, Wright M, Spiegelman BM. A cold-inducible coactivator of nuclear receptors linked to adaptive thermogenesis. *Cell*. 1998;92(6):829-839.
- Lin J, Handschin C, Spiegelman BM. Metabolic control through the PGC-1 family of transcription coactivators. *Cell Metab*. 2005;1(6):361-370.
- Tveden-Nyborg P, Bergmann TK, Jessen N, Simonsen U, Lykkesfeldt J. BCPT policy for experimental and clinical studies. *Basic Clin Pharmacol Toxicol*. 2021;128(1):4-8.
- Yin R, Guo D, Zhang S, Zhang X. miR-706 inhibits the oxidative stress-induced activation of PKC α /TAOK1 in liver fibrogenesis. *Sci Rep*. 2016;6:37509.
- Kuramitsu K, Gallo D, Yoon M, et al. Carbon monoxide enhances early liver regeneration in mice after hepatectomy. *Hepatology*. 2011;53(6):2016-2026.
- Pambianco S, Giovarelli M, Perrotta C, et al. Reversal of defective mitochondrial biogenesis in limb-girdle muscular dystrophy 2D by independent modulation of histone and PGC-1 α acetylation. *Cell Rep*. 2016;17(11):3010-3023.
- Sen N, Satija Y, Das S. PGC-1 α , a key modulator of p53, promotes cell survival upon metabolic stress. *Mol Cell*. 2011;44(4):621-634.
- Vinas J, Sola A, Hotter G. Mitochondrial NOS upregulation during renal I/R causes apoptosis in a peroxynitrite-dependent manner. *Kidney Int*. 2006;69(8):1403-1409.
- Tachibana S, Zhang X, Ito K, et al. Interleukin-6 is required for cell cycle arrest and activation of DNA repair enzymes after partial hepatectomy in mice. *Cell Biosci*. 2014;4(1):6.
- Varela-Rey M, Beraza N, Lu SC, Mato JM, Martinez-Chantar ML. Role of AMP-activated protein kinase in the control of hepatocyte priming and proliferation during liver regeneration. *Exp Biol Med (Maywood)*. 2011;236(4):402-408.
- Consalvi S, Mozzetta C, Bettica P, et al. Preclinical studies in the mdx mouse model of duchenne muscular dystrophy with the histone deacetylase inhibitor givinostat. *Mol Med*. 2013;19:79-87.

24. Minetti GC, Colussi C, Adami R, et al. Functional and morphological recovery of dystrophic muscles in mice treated with deacetylase inhibitors. *Nat Med*. 2006;12(10):1147-1150.
25. Zhang L, Liu L, He Z, et al. Inhibition of wild-type p53-induced phosphatase 1 promotes liver regeneration in mice by direct activation of mammalian target of rapamycin. *Hepatology*. 2015;61(6):2030-2041.
26. Liu WH, Zhao YS, Gao SY, et al. Hepatocyte proliferation during liver regeneration is impaired in mice with methionine diet-induced hyperhomocysteinemia. *Am J Pathol*. 2010;177(5):2357-2365.
27. Vousden KH, Prives C. Blinded by the light: the growing complexity of p53. *Cell*. 2009;137(3):413-431.
28. Bohlig L, Rother K. One function—multiple mechanisms: the manifold activities of p53 as a transcriptional repressor. *J Biomed Biotechnol*. 2011;2011:464916.
29. Fischer M, Quaas M, Steiner L, Engeland K. The p53-p21-DREAM-CDE/CHR pathway regulates G₂/M cell cycle genes. *Nucleic Acids Res*. 2016;44(1):164-174.
30. Taylor WR, Stark GR. Regulation of the G₂/M transition by p53. *Oncogene*. 2001;20(15):1803-1815.
31. Dulic V, Kaufmann W, Wilson S, et al. p53-dependent inhibition of cyclin-dependent kinase activities in human fibroblasts during radiation-induced G₁ arrest. *Cell*. 1994;76(6):1013-1023.
32. Fausto N. Liver regeneration. *J Hepatol*. 2000;32(1 Suppl):19-31.
33. Blindenbacher A, Wang X, Langer I, Savino R, Terracciano L, Heim MH. Interleukin 6 is important for survival after partial hepatectomy in mice. *Hepatology*. 2003;38(3):674-682.
34. Jin X, Zhang Z, Beer-Stolz D, Zimmers TA, Koniaris LG. Interleukin-6 inhibits oxidative injury and necrosis after extreme liver resection. *Hepatology*. 2007;46(3):802-812.
35. Diehl AM. Cytokine regulation of liver injury and repair. *Immunol Rev*. 2000;174:160-171.
36. Taub R. Liver regeneration: from myth to mechanism. *Nat Rev Mol Cell Biol*. 2004;5(10):836-847.
37. Lagoudakis L, Garcin I, Julien B, et al. Cytosolic calcium regulates liver regeneration in the rat. *Hepatology*. 2010;52(2):602-611.
38. Houten SM, Auwerx J. PGC-1 α : turbocharging mitochondria. *Cell*. 2004;119(1):5-7.
39. Ooi SL, Henikoff S. Germline histone dynamics and epigenetics. *Curr Opin Cell Biol*. 2007;19(3):257-265.
40. Allis CD, Jenuwein T. The molecular hallmarks of epigenetic control. *Nat Rev Genet*. 2016;17(8):487-500.
41. Stoll S, Wang C, Qiu H. DNA methylation and histone modification in hypertension. *Int J Mol Sci*. 2018;19(4).
42. Wang J, Qiu Z, Wu Y. Ubiquitin regulation: the histone modifying enzyme's story. *Cell*. 2018;7(9):118.
43. Ge ZJ, Schatten H, Zhang CL, Sun QY. Oocyte ageing and epigenetics. *Reproduction*. 2015;149(3):R103-R114.
44. Park S, Stanfield RL, Martinez-Yamout MA, Dyson HJ, Wilson IA, Wright PE. Role of the CBP catalytic core in intramolecular SUMOylation and control of histone H3 acetylation. *Proc Natl Acad Sci U S A*. 2017;114(27):E5335-E5342.

SUPPORTING INFORMATION

Additional supporting information may be found in the online version of the article at the publisher's website.

How to cite this article: Zhang L, Wang W, Liu L, Zhang Y, Zhang X. Peroxisome proliferator-activated receptor gamma coactivator 1-alpha protects a fibrotic liver from partial hepatectomy-induced advanced liver injury through regulating cell cycle arrest. *Basic Clin Pharmacol Toxicol*. 2022;130(2):254-267. doi:10.1111/bcpt.13697